

Original Article

# A 15-Segment Fractal Antenna Using Characteristic Mode Analysis

R. Amrutha<sup>1</sup>, R. Gayathri<sup>2</sup>

<sup>1,2</sup>Department of ECE, FEAT, Annamalai University, Tamilnadu, India.

<sup>1</sup>Corresponding Author : [amruthaammu27@gmail.com](mailto:amruthaammu27@gmail.com)

Received: 03 May 2024

Revised: 08 July 2024

Accepted: 30 July 2024

Published: 28 August 2024

**Abstract** - In this research, the Iterated Function System (IFS) concept is utilized to develop a novel 15-segment fractal antenna. Additionally, Characteristic Mode Analysis (CMA) is applied to scrutinize the electromagnetic behavior of the proposed fractal structure in a multilayer medium. This examination yields insights into the physical significance of modes present in the antenna. Based on these insights, further investigation of the surface current distribution and modal significance of the antenna is conducted to mitigate unwanted harmonics without necessitating additional filter components. The resulting modified 15-segment fractal antenna demonstrates suitability for applications in the C and X bands.

**Keywords** - Characteristic mode analysis, C band, Fractal, Iterated function system, 15-segment fractal antenna, X band.

## 1. Introduction

Fractals are geometrical structures in which identical patterns recur at gradually smaller scales. The key properties of fractal geometry [2] are its recursive nature, space filling and self-similarity [3]. Self-similarity attribute is utilized to persist the duplication in design geometry to operate in multiband. The space filling feature of fractals is applied to reduce antenna space. Koch curve, Sierpinski carpet, Tree, contour etc., are typically used fractals. S. Rani et al. [5] presented a modified Koch fractal that provides better return loss than the existing Koch curve.

In [5], a novel design with the combination of Minkowski and carpet antenna was designed for wireless application. A flexible antenna [6] with tree shaped fractal geometry is proposed to achieve dual resonance. The article [7] presented a compact dual frequency microstrip antenna by incorporating a Sierpinski carpet fractal into the traditional microstrip patch antenna. Fractal Antenna, being an irregular-shaped microstrip antenna, has a complex design procedure and a time-consuming optimization process.

Thus, it requires mathematical analysis to properly construct its recursive configuration and a deterministic design approach called Characteristic modal analysis to interpret and optimize its performance. The advancement of fractal geometry proffers various approaches for the mathematical analysis of irregular shapes [5]. The structure and recursive configuration of the fractal antenna can be constructed by a mathematical iterative process called Iterative Function System (IFS) [8,9]. CMA [10,11] in a

multilayered medium can provide physical insight into the operations of an irregular-shaped microstrip patch antenna, and it can also accurately characterize the modal current, model far field and resonant frequency of the radiating modes. John J Borchard et al. [14] used modal analysis to interpret the impedance characteristic of U-slot patch geometry. In [6,13], a detailed exploration of the logical design of the Fractal UWB MIMO antenna using modal analysis was presented.

Robert Martens et al. performed appropriate excitation of modes with the help of CMA for the MIMO antenna system [15]. The consolidated literature survey is given in Table 1. A novel 15-Segment fractal antenna with miniaturization and multiband characteristics has been disclosed in this research work. The objectives of this compendium are

- To construct a novel 15-segment fractal curve using a mathematical Iterative process called Iterative Function System.
- To design a novel 15-Segment fractal antenna using the proposed fractal curve with miniaturization and multiband characteristics, which are suitable for X and C band applications.
- To interpret the electromagnetic behavior of the proposed 15-Segment fractal antenna using a deterministic design approach called Characteristic modal analysis, resulting in the reduction of time-consuming trial and error optimization.
- To optimize the performance of the proposed fractal antenna by eliminating unwanted harmonics with the aid of Characteristic modal analysis to avoid the necessity of additional filter components.



Table 1. Consolidated summary

| Ref. No.      | Approach                    |                      | Contribution/Outcome                             |                 |           |
|---------------|-----------------------------|----------------------|--|-----------------|-----------|
|               | Mathematical Analysis (IFS) | Modal Analysis (CMA) | Band Rejection (Eliminating Harmonics) using CMA | Miniaturization | Multiband |
| Proposed work | Yes                         | Yes                  | Yes  | Yes             | Yes       |
| [4]           | Yes                         | No                   | No   | No              | Yes       |
| [5]           | Yes                         | No                   | No   | Yes             | Yes       |
| [6]           | No                          | No                   | No   | No              | Yes       |
| [7]           | No                          | No                   | No   | Yes             | Yes       |
| [12]          | No                          | Yes                  | No   | No              | No        |
| [15]          | No                          | Yes                  | No   | No              | Yes       |
| [16]          | No                          | Yes                  | No   | Yes             | Yes       |
| [17]          | Yes                         | Yes                  | No   | No              | Yes       |

### 2. Construction of Fractal Curve

The prototype of IFS is based on the set of affine transformation  $w(x,y)$  to an elementary shape. The affine transformation is defined in [18] as

$$W(x,y) = (Ax + By + E, Cx + Dy + F) \tag{1}$$

Here, A and D - Scaling operation; r - scaling factor, B and C - rotation by angles  $\theta_1$  and  $\theta_2$ , E and F - x, y co-ordinate translation.

$$A=r_1 \cos \theta_1; B=r_2 \sin \theta_2; C=r_1 \sin \theta_1; D=r_2 \cos \theta_2;$$

Consider S as an initial geometry and  $w_1, w_2, \dots, w_N$  as a set of affine transformations. Now, the new fractal curve  $W(S)$  is obtained by adopting the set of all the affine transformation functions to the initial geometry [19]. The new fractal curve  $W(S)$  can be obtained from

$$W(S) = \cup_{i=1}^N w_i(S) \tag{2}$$

Where the operator U is called as Hutchinson operator.

A 15-segment fractal curve is proposed in this dissertation to protract the convoluted length of the antenna to shift the operating frequency towards the lower side. The framework of the 15-Segment fractal instigates with a straight line, as shown in Figure 1(a). Then, the straight line is partitioned into 3 equal segments. The next stage of the construction procedure is to replace the middle segment of the straight line with two hexagon-like head structures, as illustrated in Figure 1(b).



Fig. 1 Construction of Fractal curve (a) Straight line (b) Straight line with two hexagon-like head structures (c) Proposed 15-Segment fractal curve

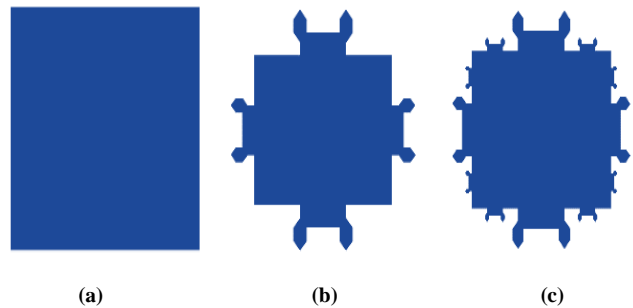


Fig. 2 Evolution of the proposed 15-Segment fractal antenna (a) Basic rectangular patch-initiator (b) Generator (c) For iteration N=2

The proposed 15-Segment fractal curve consists of three horizontal lines, six vertical lines with an indentation of  $90^\circ$  and six bent curves with an indentation of  $-45^\circ$  and  $45^\circ$  respectively. The series of affine transformation of the 15-Segment fractal curve is given in Table 2.

### 3. Design of 15-Segment Fractal Antenna

The origination of the fractal antenna, called, the initiator, is a conventional rectangular microstrip antenna. The first iteration of the 15-Segment fractal antenna is achieved by incorporating the proposed 15-Segment fractal curve, called the generator, along the four straight segments of the Euclidean initiator. This generation procedure continues up to the “N” iteration as per the requirement of the design. In this model, the 15-Segment fractal antenna is designed for the iteration  $N=2$ , as illustrated in Figure 2. The design parameters of the initiator are obtained from the transmission line model. The dimensions of the first and second iterations of the proposed 15-Segment fractal antenna are obtained from the Iterated Function System defined in section 2. A coaxial fed rectangular microstrip antenna that operates at 5.2 GHz is designed using the traditional cavity model with the parameters mentioned in Table 3.

The dimensions of the 15-Segment fractal antenna are depicted in Figure 3. The dimensions of the proposed 15-Segment fractal antenna are stated in Figure 3.

Table 2. IFS of 15-Segment fractal curve

| S. No | W(x,y)          | A      | B      | C      | D      | E      | F      |
|-------|-----------------|--------|--------|--------|--------|--------|--------|
| 1.    | W <sub>1</sub>  | 0.3    | 0      | 0      | 0.3    | 0      | 0      |
| 2.    | W <sub>2</sub>  | 0      | -0.05  | 0.05   | 0      | 0.33   | 0      |
| 3.    | W <sub>3</sub>  | -0.039 | -0.039 | 0.039  | -0.039 | 0.33   | 0.055  |
| 4.    | W <sub>4</sub>  | 0      | -0.05  | 0.055  | 0      | 0.2940 | 0.0948 |
| 5.    | W <sub>5</sub>  | 0.039  | -0.039 | 0.039  | 0.039  | 0.2940 | 0.1503 |
| 6.    | W <sub>6</sub>  | 0.039  | 0.039  | -0.039 | 0.039  | 0.33   | 0.1896 |
| 7.    | W <sub>7</sub>  | 0      | -0.05  | 0.05   | 0      | 0.3726 | 0.0948 |
| 8.    | W <sub>8</sub>  | 0.2547 | 0      | 0      | 0.2547 | 0.3726 | 0.0948 |
| 9.    | W <sub>9</sub>  | 0      | -0.05  | 0.05   | 0      | 0.6273 | 0.0948 |
| 10.   | W <sub>10</sub> | 0.039  | -0.039 | 0.039  | 0.039  | 0.2940 | 0.1503 |
| 11.   | W <sub>11</sub> | 0.039  | 0.039  | -0.039 | 0.039  | 0.66   | 0.05   |
| 12.   | W <sub>12</sub> | 0      | -0.05  | 0.05   | 0      | 0.705  | 0.1503 |
| 13.   | W <sub>13</sub> | 0.039  | -0.039 | 0.039  | 0.039  | 0.66   | 0.055  |
| 14.   | W <sub>14</sub> | 0      | -0.05  | 0.05   | 0      | 0.66   | 0      |
| 15.   | W <sub>15</sub> | 0.33   | 0      | 0      | 0.33   | 0.66   | 0      |

Table 3. Design parameters of rectangular

| S. No | Parameter                       | Dimension (mm) |
|-------|---------------------------------|----------------|
| 1.    | Ground width (w <sub>g</sub> )  | 35.44          |
| 2.    | Ground length (L <sub>g</sub> ) | 26.24          |
| 3.    | Patch width (W)                 | 17.72          |
| 4.    | Patch length (L)                | 13.12          |
| 5.    | Substrate thickness (h)         | 1.6            |
| 6.    | Dielectric constant (ε)         | 4.3            |
| 7.    | Conductor height (t)            | 0.035          |

Table 4. Performance metrics of 2<sup>nd</sup> iterated 15-Segment fractal antenna

| Frequency (GHz) | S <sub>11</sub> (dB) | BW (MHz) | VSWR | GAIN (dBi) | IMP Ω |
|-----------------|----------------------|----------|------|------------|-------|
| 4.22            | -33.1                | 163.3    | 1.04 | 3.937      | 51    |
| 6.28            | -11.6                | 80.2     | 1.71 | 1.706      | 79    |
| 11.72           | -15.2                | 259.6    | 1.42 | 5.425      | 52    |

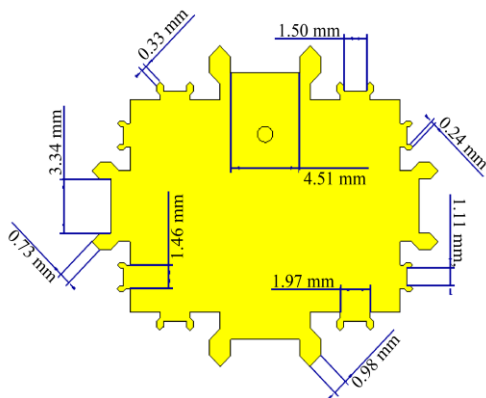


Fig. 3 Dimensions of the proposed 15 Segment fractal antenna for iteration N=2

#### 4. Driven Simulation of 15-Segment Fractal Antenna

The proposed 15-Segment antenna depicted in Figure 3 is simulated using an EM simulation tool, and its performance is

observed in terms of S<sub>11</sub>, VSWR, gain, directivity and bandwidth. The proposed 2<sup>nd</sup> iterated 15-Segment fractal antenna is investigated within the frequency range (3-13) GHz. From Figure 4, it is evident that the antenna resonates at 3 different frequencies, namely 4.22GHz, 6.28GHz and 11.72GHz, with the reflection coefficients of -33.1dB, -11.6dB and -15.2dB. Table 4 provides the performance metrics of the 2<sup>nd</sup> iterated 15-Segment fractal antenna with respect to Gain, directivity, VSWR and Bandwidth. From the results, it has been observed that the performance of the antenna at frequency f=6.28GHz is unsatisfactory.

#### 5. Characteristic Modal Analysis

CMA generates a set of current patterns that naturally present on an arbitrary structure at a distinct frequency [20]. These sets of current patterns are nothing but the modes that radiate their corresponding characteristic modal pattern independently. For a distinct frequency, an infinite number of modes can be generated [21]. Among them, few might be closer to their natural resonance and upon excitation, it will radiate significantly but the other modes may be away from their natural resonance, and as a result, they radiate less power and store more energy. The parameters that are involved in describing the characteristic mode analysis of the antenna structure are eigen value, characteristic angle and modal significance. Mathematically, the Eigenvalue [22,23] λ<sub>n</sub> is defined as the ratio of reactive power to the radiated power wherein the physical interpretation involved is that the magnitude of the eigenvalue is proportional to the total stored field energy within the radiation. Modal significance [22,23], along with modal excitation coefficient, quantifies the involvement of each mode in the total electromagnetic response to a given source. Modal Significance (MS) can be calculated from

$$MS = |1/(1+j\lambda_n)| \tag{3}$$

Further modal significance is also helpful in identifying.

### 6. Optimization of 2<sup>nd</sup> Iterated 15-Segment Fractal Antenna Using Characteristic Modal Analysis

Characteristic modal analysis for a 15-Segment fractal antenna in a multilayered medium is carried out using an EM simulation tool. In order to perform modal analysis, excitation of the antenna is removed, and all the lossy material involved in the antenna construction is converted into lossless material. The perfect conducting body and its corresponding mesh view of the proposed antenna are shown in Figure 5.

From the  $S_{11}$  response of the 2<sup>nd</sup> iterated 15-Segment antenna, it is evident that the antenna has a resonance at three different frequencies, namely 4.22GHz, 6.28GHz and 11.72GHz. Now, modal analysis is done for these frequencies separately to analyse the physical behaviour of the 15-Segment fractal antenna.

First, the resonant behaviour of the 15-segment fractal antenna is examined at a frequency (f) 4.22GHz by sorting the multimode solver. At  $f=4.22$ GHz, two modes are generated, and their corresponding eigen value, modal significance and characteristic angle are obtained, as given in Figure 6. The physical interpretation of the modal analysis at 4.22GHz is elaborated in Table 5.

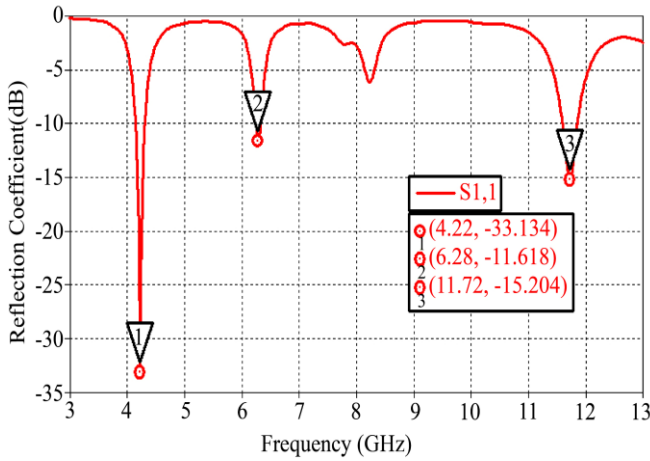


Fig. 4  $S_{11}$  characteristic of 2<sup>nd</sup> iterated 15-Segment fractal antenna

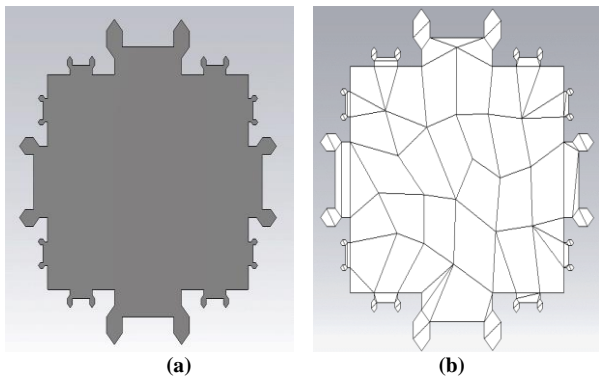


Fig. 5 15-Segment fractal antenna without feed (a) Lossless patch (b) Mesh partition into characterized modes

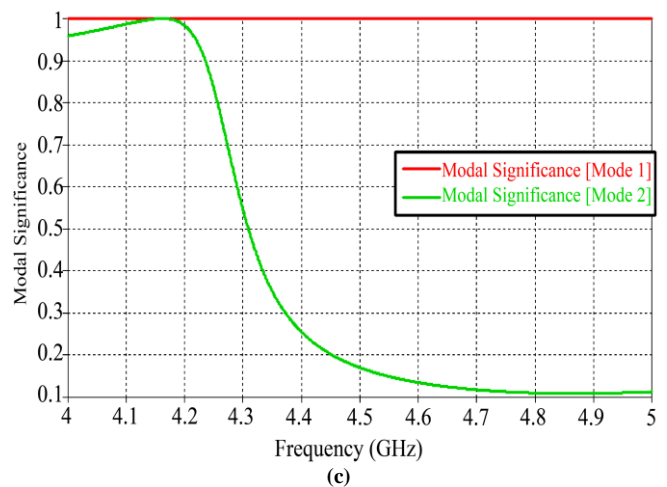
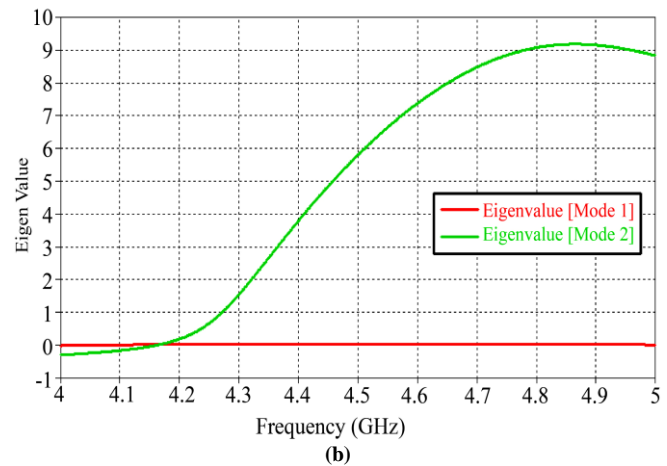
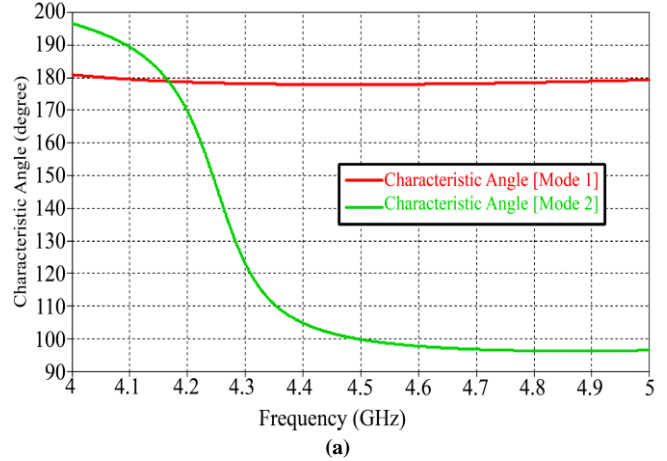


Fig. 6 CMA Parameters at  $f=4.22$  (a) Characteristic angle (b) Eigen values (c) Modal significance

Table 5. Resonant behaviour of 15-Segment fractal antenna at  $f=4.22$ GHz

| Mode | $\alpha_n$ | $\lambda_n$ | MS   | Mode Nature        |
|------|------------|-------------|------|--------------------|
| 1    | 178°       | 0.0         | 0.99 | Close to Resonance |
| 2    | 161°       | 0.3         | 0.94 | Inductive mode     |

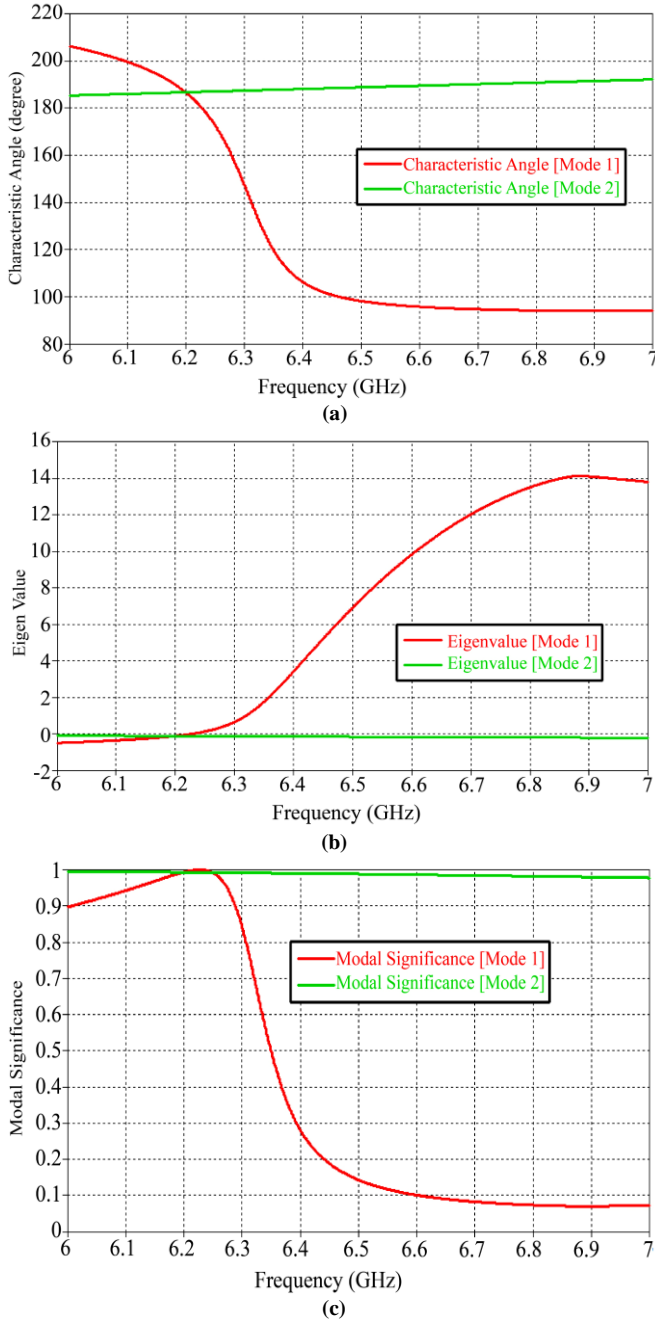


Fig. 7 CMA Parameters at f=6.28 (a) Characteristic angle (b) Eigenvalues (c) Modal significance

Mode 1 and 2 are the current patterns of the 15-Segment fractal antenna that naturally exist at f=4.22GHz. According to the CMA parametric results shown in Figure 6, the actual resonant frequencies of mode 1 and mode 2 are observed at 4.0585 GHz and 4.1625 GHz, respectively. At these frequencies, the modal parameters of the proposed antenna are exactly equivalent to the resonance condition.

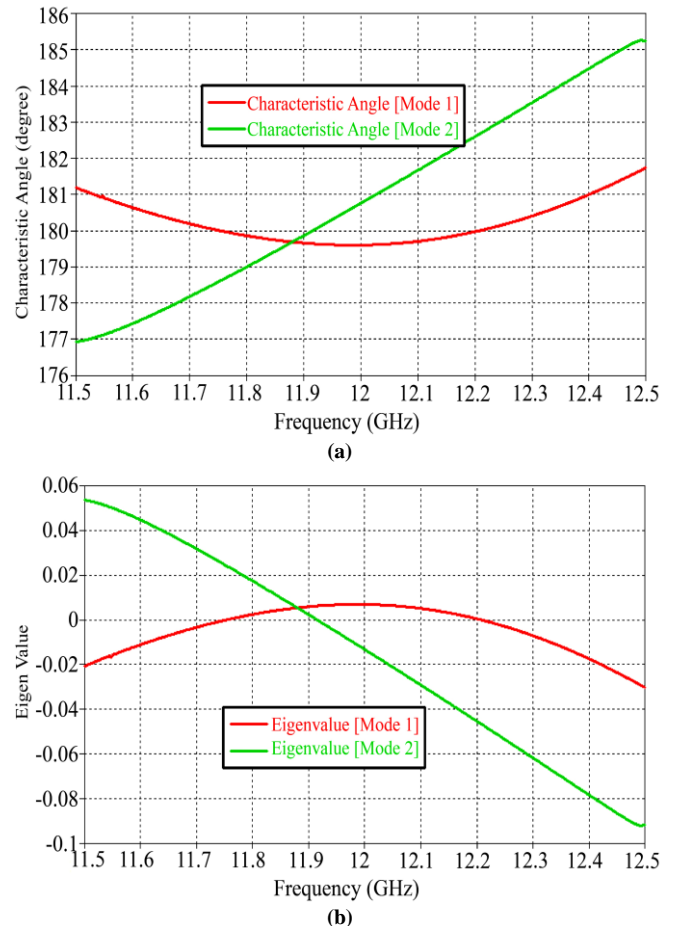
$$(i.e.) \alpha_n = 180^0; \lambda_n = 0; MS = 1$$

Now, the resonant behaviour of the proposed antenna at a frequency of 6.28GHz is analysed. At f=6.28GHz, two modes

are instigated, and their corresponding eigenvalue, modal significance and characteristic angle are obtained, as given in Figure 7. The physical interpretation of the modal analysis at 6.28GHz is presented in Table 6. Modes 1 and 2 are the current patterns of the 15-Segment fractal antenna that naturally exist at f=6.28GHz. In accordance with the CMA parametric results shown in Figure 7, it is observed that mode 1 does not contribute any significant resonance, whereas mode 2 contributes at a frequency of 6.2275 GHz. At this frequency, the modal parameters of the proposed antenna are exactly equivalent to the resonance condition. (i.e.)  $\alpha_n = 180^0; \lambda_n = 0; MS = 1$ . Finally, the resonant behaviour of the proposed antenna is examined at a frequency of 11.72GHz. At f=11.72GHz, two modes are excited, and their corresponding eigenvalue, modal significance and characteristic angle are obtained as given in Figure 8. The physical interpretation of the modal analysis at 11.72GHz is elaborated in Table 7.

Table 6. Resonant behaviour of 15-Segment fractal antenna at f=6.28GHz

| Mode | $\alpha_n$       | $\lambda_n$ | MS   | Mode Nature          |
|------|------------------|-------------|------|----------------------|
| 1    | 158 <sup>0</sup> | 0.3         | 0.93 | Non-Significant mode |
| 2    | 187 <sup>0</sup> | -0.1        | 0.94 | Non-Significant mode |





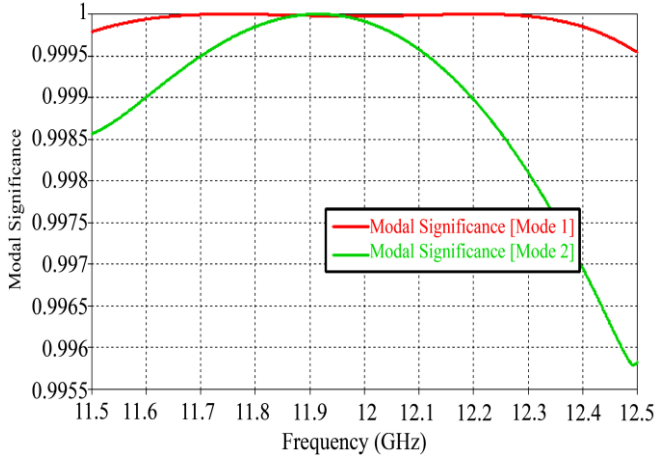


Fig. 8 CMA Parameters at f=11.72 (a) Characteristic angle (b) Eigenvalues (c) Model significance

Table 7. Resonant behaviour of 15-Segment fractal antenna at f=11.72GHz

| Mode | $\alpha_n$ | $\lambda_n$ | MS   | Mode Nature        |
|------|------------|-------------|------|--------------------|
| 1    | $180^0$    | 0.00        | 0.99 | Resonance Mode     |
| 2    | $178^0$    | 0.02        | 0.99 | Close to resonance |

Modes 1 and 2 are the current patterns of the 15-segment fractal antenna that naturally exist at f=11.72GHz. According to the CMA parametric results shown in Figure 8, the actual resonant frequencies of mode 1 and mode 2 are observed at 11.7545 GHz and 11.9155 GHz, respectively. At these frequencies, the modal parameters of the proposed antenna are exactly equivalent to the resonance condition. (i.e.)  $\alpha_n = 180^0$ ;  $\lambda_n = 0$ ; MS=1. The overall physical interpretation of the modal analysis done at the resonant frequencies of 2<sup>nd</sup> iterated 15-segment fractal antenna is discussed as follows:

6.1. At 4.22GHz

The excited modes 1 and 2 do not exactly satisfy the resonance condition at f=4.22GHz. The natural resonant frequencies of modes 1 and 2 existing at the structure are 4.0585 and 4.1625 GHz, respectively. The band of the resonating frequency (f=4.22GHz) observed from the S<sub>11</sub> plot of the 2<sup>nd</sup> iterated 15-Segment fractal antenna is (4.14 – 4.30) GHz.

The natural resonating frequency of mode 2 falls within the band of 4.22GHz, whereas mode 1 is 90MHZ away from the band. Therefore, the first resonating band corresponding to f=4.22GHz should be slightly shifted towards the left side such that it covers the frequency 4.0585GHz.

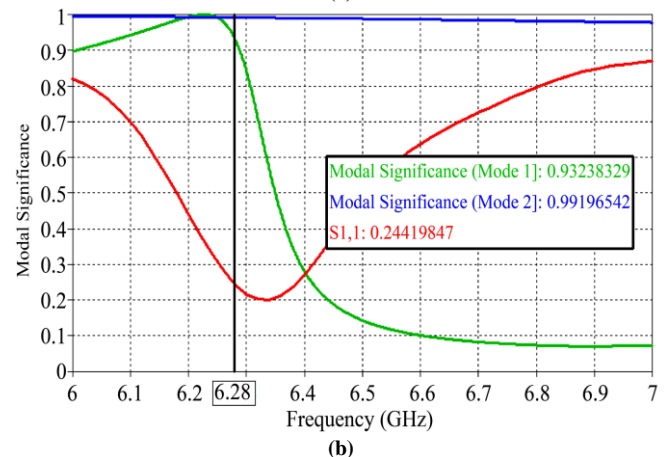
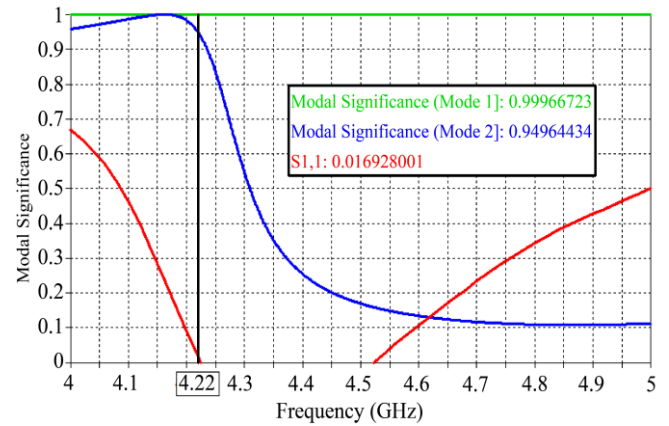
6.2. At 6.28GHz

Both the modes excited at this resonant frequency are inefficient modes, so this band should be removed.

6.3. At 11.72GHz

At 11.72GHz, the excited modes are very close to the resonance condition. The natural resonant frequencies of modes 1 and 2 existing at the structure are 11.75 and 11.91 GHz, respectively. The band of the resonating frequency (f=11.72GHz) observed from the S<sub>11</sub> plot of the 2<sup>nd</sup> iterated 15-Segment fractal antenna is (11.59-11.90) GHz. The natural resonating frequency of both modes falls within the band of 11.72GHz. Therefore, no changes are required in this band.

Surface current distribution of the modes at distinct frequencies plays a major role in the optimization of the proposed antenna. While performing CMA analysis, each frequency is excited with two different modes. It is necessary to identify the most significant mode among them. This is because the surface current distribution of the most significant mode that corresponds to the resonating frequency is enough to improve the performance of the antenna. The most significant mode is located by comparing the S<sub>11</sub> of the proposed antenna obtained from driven simulation with the modal significance obtained from Characteristic modal analysis. A comparison plot of S<sub>11</sub> with modal significance is given in Figure 9. From the results shown in Figure 9, the most significant mode of the resonating frequencies is identified and listed in Table 8.



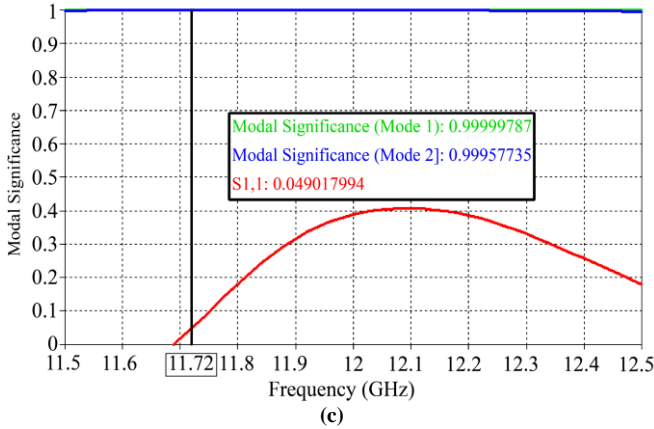


Fig. 9 Comparison plot of  $S_{11}$  with modal significance (a) at  $f=4.22$ GHz (b) at  $f=6.28$ GHz (c) at  $f=11.72$

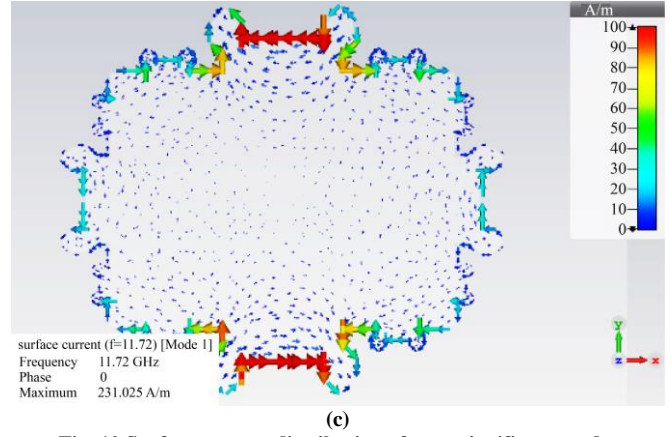


Fig. 10 Surface current distribution of most significant modes (a) at  $f=4.22$ GHz (b) at  $f=6.28$ GHz (c) at  $f=11.72$

Table 8. Most significant mode

| f (GHz) | Mode | Modal significance value | Most significant mode |
|---------|------|--------------------------|-----------------------|
| 4.22    | 1    | 0.99                     | Mode 1                |
|         | 2    | 0.94                     |                       |
| 6.28    | 1    | 0.93                     | Mode 2                |
|         | 2    | 0.99                     |                       |
| 11.72   | 1    | 0.99                     | Mode 1                |
|         | 2    | 0.95                     |                       |

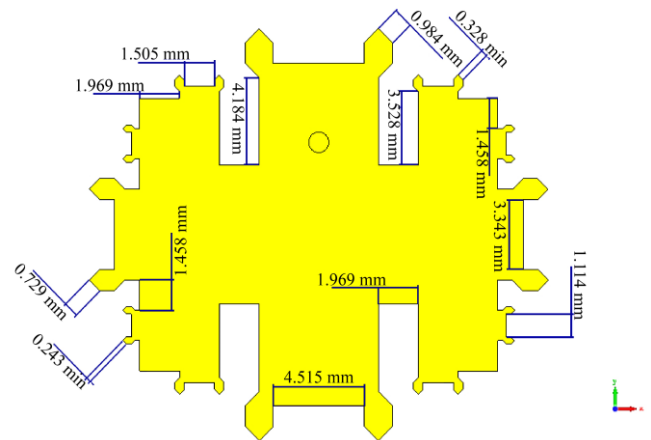
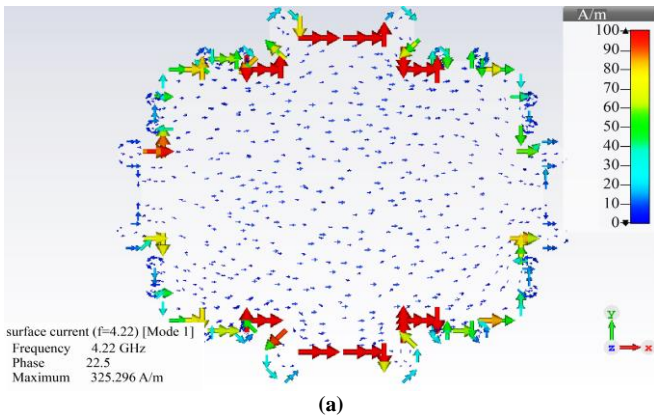
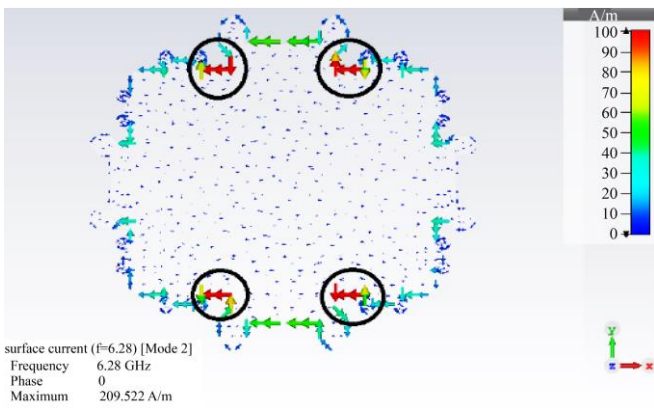


Fig. 11 Modified 15-Segment fractal antenna



(a)



(b)

Now, the surface current distribution of the most significant modes illustrated in Figure 10 is analyzed to optimize the performance of the 2<sup>nd</sup> iterated 15-Segment fractal antenna. For all the frequencies, modal currents are strongly concentrated at the vertices of the fractal element. The purpose of the analysis of surface current distribution is to remove the band existing at  $f=6.28$ GHz. In order to achieve this, mode 2 should be tuned independently. The spotted region in Figure 10(b) is where the current is high in surface distribution. Therefore, incorporating changes in that region will affect mode 2, which in turn contributes to the removal of the band at  $f=6.28$ . Four capacitive slots are included in that spotted region to influence the performance of mode 2. The dimension of each slot is  $1.96 \times 3.2$ mm. The modified structure of the 2<sup>nd</sup> iterated 15-Segment fractal antenna is shown in Figure 11.

### 7. Half Mode Analysis of Modified 15-Segment Fractal Antenna

Half mode analysis is carried out to validate the self-symmetry nature of the modified 15-Segment fractal antenna. This analysis is done by eliminating one side of the resonator [24,25], as shown in Figure 12. Generally, in half mode

analysis, additional shorting in the form of pins or via adding with a half patch to introduce Defected structure. But here, no such external pin or via is included as the proposed antenna is a fractal and it is defected by nature itself. Now, the half patch is coaxially fed and simulated using an EM simulator. Since the overall size of the antenna is reduced to half of its size, the modified 15-Segment fractal antenna will now operate in quarter wave transmission mode, and it is approximated as PMC (Perfectly Magnetic Conducting). It implies that the inner electric field only has a vertical component, and thus, only TMX modes exists in the considered part of the resonator.

The reflection coefficient plot of the modified 15-Segment fractal antenna in half mode analysis is illustrated in Figure 13. From Figure 13, it is evident that the half patch antenna resonates at three different frequencies, namely 4.4GHz, 4.9GHz and 6.4GHz with the reflection coefficient of -23.8dB, -23.3dB and -14.6dB. The basic initiator for the proposed antenna is a traditional rectangular patch antenna, which is designed for the frequency  $f=5.2$ GHz. Therefore, the baseband for the modified 15-Segment fractal antenna is 5.2GHz, and it is achieved in the coverage of the second band. The notches present in the left side of the fractal will induce friction effect to the structure, and also the current will not be evenly distributed as only half of the patch is considered. Under these circumstances, cyclic simulation takes place, and the frequency gets tuned to one step below the baseband. This contributes to the resonance at 4.4GHz. The last resonance observed at frequency  $f=6.4$ GHz is a harmonic that occurs due to the imbalance in the structure. Now, the full patch, which is the modified 15-Segment fractal antenna presented in Figure 11, is considered for further analysis. The antenna mentioned above is simulated using EM simulation software. The prototype of the proposed antenna is fabricated to measure its return loss using a vector analyzer and radiation pattern using an anechoic chamber. The fabricated prototype and its measurement setup are shown in Figure 14. The comparison of simulated parameters with the measured results of the modified 15-Segment fractal antenna is shown in Table 9, and the graphical representation of the return loss comparison is displayed in Figure 15.

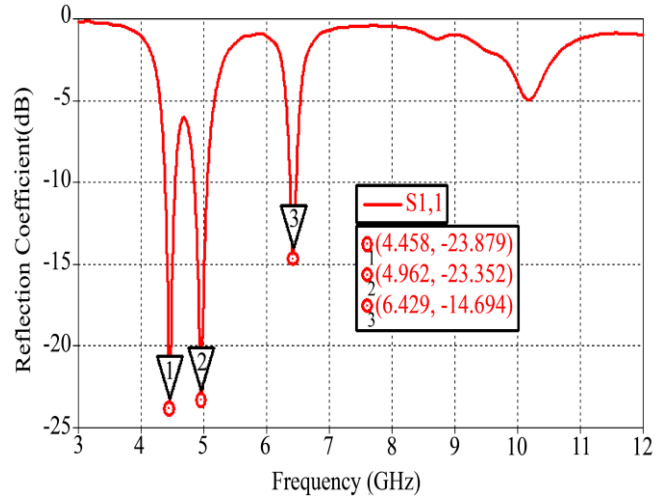


Fig. 13  $S_{11}$  characteristic of a modified 15-Segment fractal antenna in half mode analysis

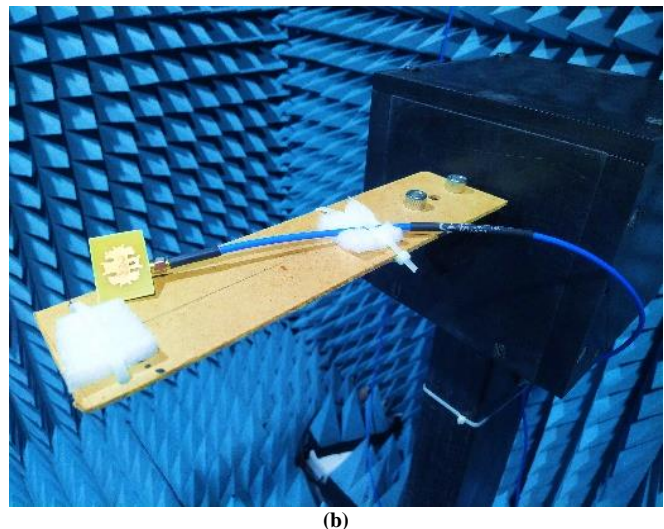
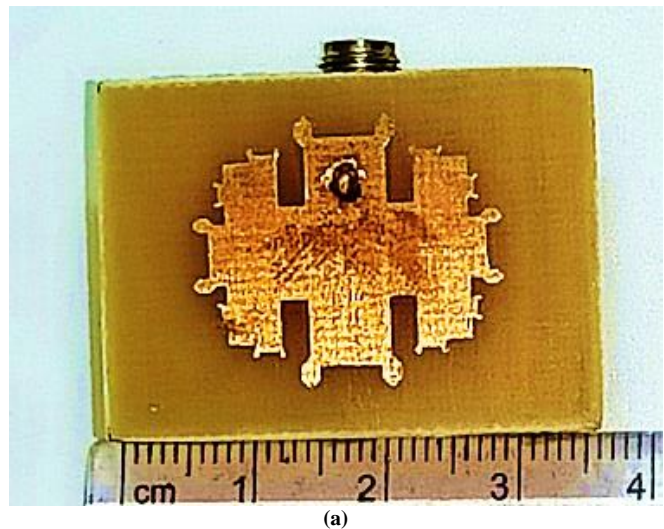


Fig. 14 (a) Fabricated prototype of a modified 15-Segment fractal antenna (b) Measurement setup

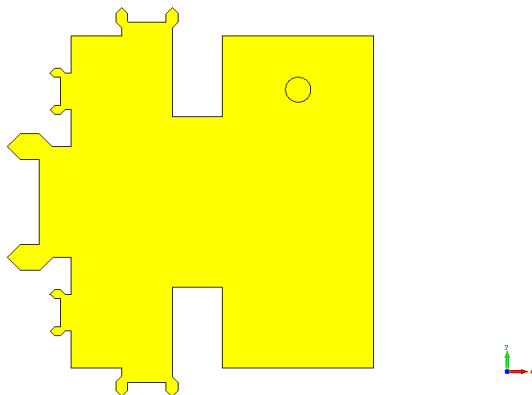


Fig. 12 Half mode analysis of modified 15-Segment fractal antenna



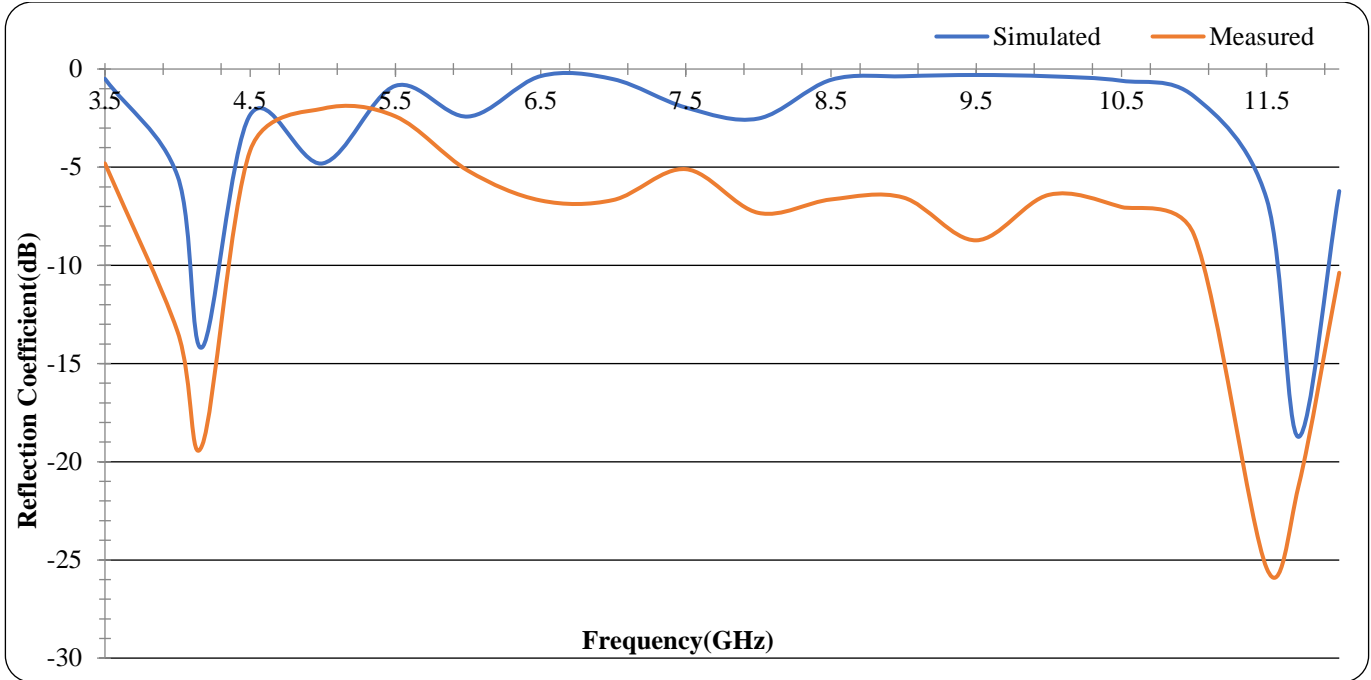


Fig. 15 Simulated vs Measured return loss plot of modified 15-Segment fractal antenna

From Figure 15, it is observed that the modified 15-Segment fractal antenna resonates at two different frequencies, namely 4.14GHz and 11.74GHz, with the reflection co efficient of -17.43dB and -18.8 dB.

When the full patch is considered, the four capacitive slots present in the structure provide a proper frequency balance between the left and right-side notches present in the fractal. This balance removes harmonics, produces circular electric transmission and also distributes power equally in the structure.

As a consequence of the above frequency balance, two resonances have been observed at frequencies  $f=4.14\text{GHz}$  and  $f=11.72\text{GHz}$ , respectively.

The first resonating band,  $\text{TM}_{01}$ , is the lower band that occurs one step below the baseband, and the second resonating band,  $\text{TM}_{10}$ , is the upper band that exhibits resonance at two times the frequency of the baseband. Thus, the right-side patch replicates the mirror function of the left side patch, which validates the self-symmetry nature of the proposed fractal antenna and, by also placing the capacitive slot at the right spot using CMA, contributes to the removal of non-significant mode present at frequency  $f=6.28\text{GHz}$ .

The surface current distribution of the modified 15-Segment fractal antenna is given in Figure 16. The maximum current density is observed at the edges of the capacitive slots for frequency  $f=4.14\text{GHz}$  and at the major notches present along the width of the patch for  $f=11.72\text{GHz}$ .

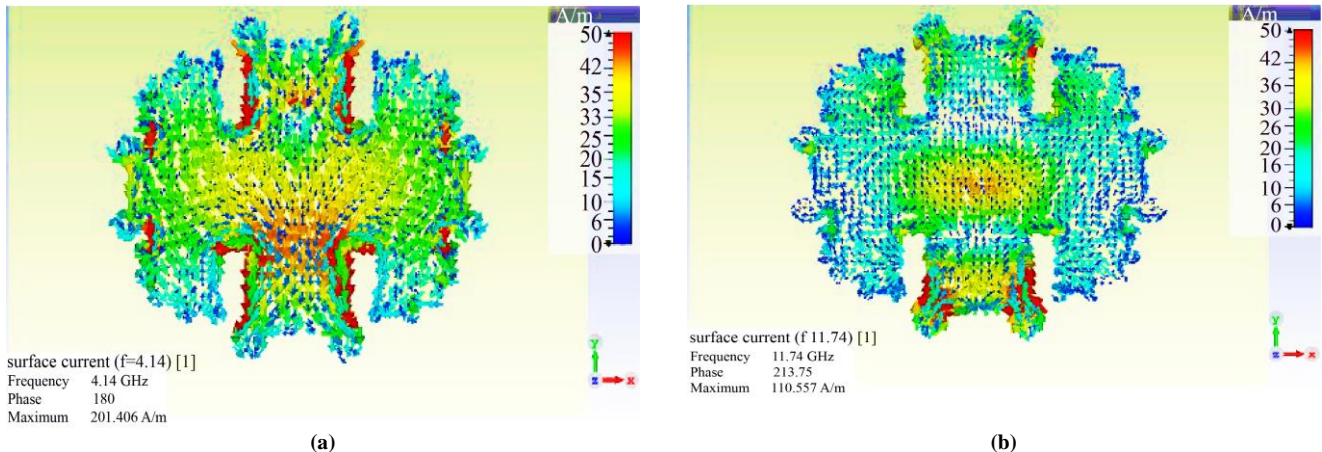


Fig. 16 Surface current distribution of modified 15-Segment fractal antenna at (a) $f=4.14\text{GHz}$  (b) $f=11.74\text{GHz}$

**Table 9. Simulated vs Measured parameters of modified 15-Segment fractal antenna**

| Parameter                    | Band 1    |          | Band 2    |          |
|------------------------------|-----------|----------|-----------|----------|
|                              | Simulated | Measured | Simulated | Measured |
| Resonant frequency (GHz)     | 4.14      | 4.17     | 11.72     | 11.5     |
| Return loss (dB)             | -17.43    | -19.15   | -18.88    | -25.42   |
| VSWR                         | 1.31      | 1.237    | 1.25      | 1.060    |
| Gain (dBi)                   | 3.239     | 3.752    | 5.530     | 3.628    |
| Input Impedance ( $\Omega$ ) | 41        | 47       | 43        | 47       |
| Bandwidth (MHz)              | 148       | 356      | 290       | 681      |

**Table 10. Comparison with prior art**

| Ref No        | Fractal Type                           | Resonating Band/frequency (GHz) | Gain (dBi)       | Application              |
|---------------|--|---------------------------------|------------------|--------------------------|
| [26]          | Cross slotted fractal antenna          | (2.41-2.57)<br>(3.9-4.11)       | Peak gain of 3.2 | Wi-Fi                    |
| [27]          | SRR inspired fractal antenna           | (3.01-4.18)<br>(1.75-2)         | 1.5<br>2.05      | GSM                      |
| [28]          | L slot fractal                         | (10.26-12.13)<br>(16GHz-18.23)  | 7.1              | X and Ku band            |
| [29]          | Sierpnski Carpet based fractal         | 11.16<br>17.16                  | 6                | X and Ku band            |
| [30]          | Arrow cross shape fractal              | 3.2<br>4.8                      | 2.96<br>3.47     | Wi-Fi,<br>Wi-MAX<br>WLAN |
| [31]          | Minkowski like fractal                 | 4.4<br>6.1                      | 3.8<br>6.2       | Wireless Communication   |
| [1]           | Combined Minkowski – Sierpinski carpet | 4<br>5.9                        | 0.4<br>6.2       | Satellite Applications   |
| Proposed Work | 15-Segment fractal antenna             | 4.14<br>11.72                   | 3.239<br>5.530   | C and Ku band            |

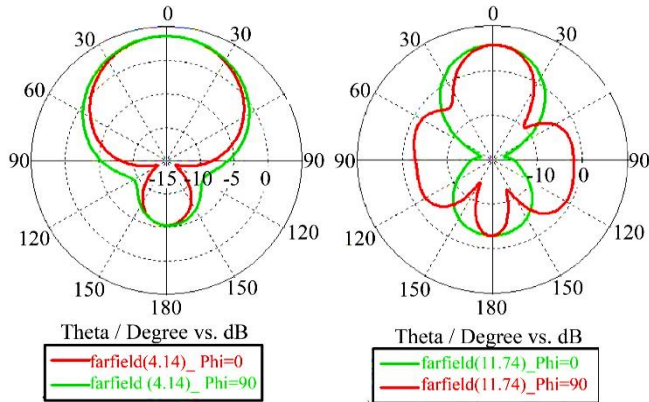


**Fig. 17 Radiation pattern of modified 15-Segment fractal antenna at (a) f=4.14GHz (b)f=11.74GHz**

Figure 17 depicts the radiation pattern of the proposed antenna. From Figure 15 and Table 9, it is apparent that the measured results are actually better than the simulated results. This deviation from the simulated result might be due to the antenna fabrication, which is not 100% equal to the simulated dimensions or imperfections involved in the soldering of the SMA connector. The comparative exploration of the proposed work with the prior art [26-32] is given in Table 10.

### 8. Conclusion

Designing a fractal antenna using a deterministic design approach will minimize the time-consuming trial and error optimizations. In this work, a 15-segment fractal antenna up to the second iteration is designed and optimized using Characteristic mode analysis. The optimized antenna exhibits dual resonance at frequencies 4.14GHz and 11.72GHz, respectively, with good return loss, gain, directivity, VSWR, bandwidth and input impedance.

The measurement of the fabricated prototype shows better results than the simulated module. Thus, a perfect design of a 15-Segment fractal antenna has been achieved for C and X band applications with size reduction and dual band characteristics. From the overall analysis, the following contemplations are evident.

- (a) As the number of iterations of the fractal increases, the resonating band shifts towards the left side. Thereby leading towards the miniaturization of the proposed 15-Segment fractal antenna.
- (b) The proposed antenna is proven to have self-similar behaviour. This characteristic of the fractal antenna contributes towards its dual band operation.

(c) The Modified 15-Segment fractal antenna eliminates unwanted harmonics using a deterministic design approach called Characteristic Mode Analysis. This avoids the necessity of additional filter components.

(d) The Modified 15-Segment fractal antenna resonates at two different frequencies, namely  $f=4.14\text{GHz}$  and  $11.74\text{GHz}$ , with a peak gain of  $3.239\text{dBi}$  and  $5.530\text{dBi}$ , respectively.

In addition, the proposed antenna also shows a steady radiation pattern, VSWR, directivity, return loss and input impedance. Thus, it is a suitable design for C and X band applications.

## Conflicts of Interest

- All authors have participated in (a) conception and design, analysis and interpretation of the data; (b) drafting the article or revising it critically for important intellectual content; and (c) approval of the final version.
- This manuscript has not been submitted to, nor is it under review at, another journal or other publishing venue.
- The authors have no affiliation with any organization with a direct or indirect financial interest in the subject matter discussed in the manuscript.
- The authors have affiliations with organizations with direct or indirect financial interest in the subject matter discussed in the manuscript.

## References

- [1] Arshad Karimbu Vallappil et al., "Dual-Band Minkowski–Sierpinski Fractal Antenna for Next Generation Satellite Communications and Wireless Body Area Networks," *Microwave and Optical Technology Letter*, vol. 60, no. 1, pp. 171-178, 2018. [[CrossRef](#)] [[Google Scholar](#)] [[Publisher Link](#)]
- [2] Michael F. Barnsley, *Fractals Everywhere*, Academic Press Professional, pp. 1-565, 1993. [[Google Scholar](#)] [[Publisher Link](#)]
- [3] J.P. Gianvittorio, and Y. Rahmat-Samii, "Fractal Antennas: A Novel Antenna Miniaturization Technique, and Applications," *IEEE Antenna and Propagation Magazine*, vol. 44, no. 1, pp. 20-36, 2002. [[CrossRef](#)] [[Google Scholar](#)] [[Publisher Link](#)]
- [4] Jaime Anguera et al., "Fractal Antennas: An Historical Perspective," *Fractal and Fractional*, vol. 4, no. 1, pp. 1-26, 2020. [[CrossRef](#)] [[Google Scholar](#)] [[Publisher Link](#)]
- [5] S. Rani, and A.P. Singh, "On the Design and Analysis of Modified Koch Curve Fractal Antenna," *Journal of the Institution of Engineers (India): Series B*, vol. 94, pp. 231-236, 2013. [[CrossRef](#)] [[Google Scholar](#)] [[Publisher Link](#)]
- [6] Narinder Sharma, Vipul Sharma, and Sumeet Singh Bhatia, "A Novel Hybrid Fractal Antenna for Wireless Applications," *Progress In Electromagnetics Research M*, vol. 73, pp. 25-35, 2018. [[CrossRef](#)] [[Google Scholar](#)] [[Publisher Link](#)]
- [7] Aya N. Alkhafaji, Sinan M. Abdulsatar, and awad Kadhim Ali, "Design of Flexible Dual-Band Tree Fractal Antenna for Wearable Applications," *Progress in Electromagnetics Research C*, vol. 125, pp. 51-66, 2022. [[CrossRef](#)] [[Google Scholar](#)] [[Publisher Link](#)]
- [8] Sika Shrestha, Seong Ro Lee, and Dong-You Choi, "A New Fractal-Based Miniaturized Dual Band Patch Antenna for RF Energy Harvesting," *International Journal of Antennas and Propagation*, vol. 2014, no. 1, pp. 1-9, 2014. [[CrossRef](#)] [[Google Scholar](#)] [[Publisher Link](#)]
- [9] Jawad Ali et al., "Cantor Fractal-Based Printed Slot Antenna for Dual-Band Wireless Applications," *International Journal of Microwave and Wireless Technologies*, vol. 8, no. 2, pp. 263-270, 2016. [[CrossRef](#)] [[Google Scholar](#)] [[Publisher Link](#)]
- [10] Jawad K. Ali, and Emad S. Ahmed, "A New Fractal Based Printed Slot Antenna for Dual Band Wireless Communication Applications," *Proceedings of Progress in Electromagnetics Research Symposium*, Kuala Lumpur, Malaysia, pp. 1518-1521, 2012. [[Google Scholar](#)] [[Publisher Link](#)]
- [11] Yikai Chen, and Chao-Fu Wang, *Characteristic Modes: Theory and Applications in Antenna Engineering*, John Wiley & Sons, New jersey, 2015. [[CrossRef](#)] [[Google Scholar](#)] [[Publisher Link](#)]
- [12] Marta Cabedo-Fabres et al., "The Theory of Characteristic Modes Revisited: A Contribution to the Design of Antennas for Modern Applications," *IEEE Antennas and Propagation Magazine*, vol. 49, no. 5, pp. 52-68, 2007. [[CrossRef](#)] [[Google Scholar](#)] [[Publisher Link](#)]
- [13] Asutosh Mohanty, and Bikash Ranjan Behera, "Characteristics Mode Analysis: a Review of Its Concepts, Recent Trends, State-of-the-Art Developments and its Interpretation with a Fractal UWB MIMO Antenna," *Progress in Electromagnetics Research B*, vol. 92, pp. 19-45, 2021. [[CrossRef](#)] [[Google Scholar](#)] [[Publisher Link](#)]
- [14] John J. Borchardt, and Tyler C. Lapointe, "U-Slot Patch Antenna Principle and Design Methodology Using Characteristic Mode Analysis and Coupled Mode Theory," *IEEE Access*, vol. 7, pp. 109375-109385, 2019. [[CrossRef](#)] [[Google Scholar](#)] [[Publisher Link](#)]
- [15] Robert Martens, and Dirk Manteuffel, "Systematic Design Method of a Mobile Multiple Antenna System Using the Theory of Characteristic Modes," *IET Microwaves, Antennas & Propagation*, vol. 8, no. 12, pp. 887-893, 2014. [[CrossRef](#)] [[Google Scholar](#)] [[Publisher Link](#)]
- [16] Dilaawaiz Fazal, and Mojeeb Bin Ihsan, "Analysis of Partial Koch Fractal Antenna Using Characteristic Mode Theory," *2019 8<sup>th</sup> Asia-Pacific Conference on Antennas and Propagation*, Incheon, Korea (South), pp. 389-390, 2019. [[CrossRef](#)] [[Google Scholar](#)] [[Publisher Link](#)]

- [17] Guorui Han, Zijun Zheng, and Wenmei Zhang, "A Low-Profile Dual-Band Antenna Using Fractal-Based Wideband Metasurface with Stable Radiation Pattern," *International Journal of RF and Microwave Computer-Aided Engineering*, 2022. [[CrossRef](#)] [[Google Scholar](#)] [[Publisher Link](#)]
- [18] Geeta B. Kalkhambkar, Rajashri Khanai, and Pradeep Chindhi, "Design and Characteristics Mode Analysis of a Cantor Set Fractal Monopole Antenna for IoT Applications," *Progress in Electromagnetics Research C*, vol. 119, pp. 161-175, 2022. [[CrossRef](#)] [[Google Scholar](#)] [[Publisher Link](#)]
- [19] Benoit B. Mandelbrot, *The Fractal Geometry of Nature*, Henry Holt and Company, pp. 1-468, 1983. [[Google Scholar](#)] [[Publisher Link](#)]
- [20] Wojciech Jan Krzysztofik, *Fractals in Antennas and Metamaterials Applications*, IntechOpen, 2017. [[Google Scholar](#)] [[Publisher Link](#)]
- [21] R. Harrington, and J. Mautz, "Theory of Characteristic Modes for Conducting Bodies," *IEEE Transactions on Antennas and Propagation*, vol. 19, no. 5, pp. 622-628, 1971. [[CrossRef](#)] [[Google Scholar](#)] [[Publisher Link](#)]
- [22] R. Harrington, J. Mautz, and Yu Chang, "Characteristic Modes for Dielectric and Magnetic Bodies," *IEEE Transactions and Antennas Propagation*, vol. 20, no. 2, pp. 194-198, 1972. [[CrossRef](#)] [[Google Scholar](#)] [[Publisher Link](#)]
- [23] R. Harrington, and J. Mautz, "Computation of Characteristic Modes for Conducting Bodies," *IEEE Transactions on Antennas and Propagation*, vol. 19, no. 5, pp. 629-639, 1971. [[CrossRef](#)] [[Google Scholar](#)] [[Publisher Link](#)]
- [24] Martin Vogel et al., "Characteristic Mode Analysis: Putting Physics back into Simulation," *IEEE Antennas and Propagation Magazine*, vol. 57, no. 2, pp. 307-317, 2015. [[CrossRef](#)] [[Google Scholar](#)] [[Publisher Link](#)]
- [25] Feng-Xue Liu et al., "Wearable Applications of Quarter-Wave Patch and Half-Mode Cavity Antennas," *IEEE Antennas and Wireless Propagation Letters*, vol. 14, pp. 1478-1481, 2015. [[CrossRef](#)] [[Google Scholar](#)] [[Publisher Link](#)]
- [26] Shahid Irfan, Thalakituna Dushmantha, and Heimlich Michael, "Novel Half-Patch Based 1-D Periodic Structure with Better Control over Stop Bandwidth," *2019 IEEE Asia-Pacific Microwave Conference*, Singapore, pp. 1712-1714, 2019. [[CrossRef](#)] [[Google Scholar](#)] [[Publisher Link](#)]
- [27] Ram Krishan, *A Novel Cross-Slotted Dual-Band Fractal Microstrip Antenna Design for Internet of Things (IoT) Applications*, 1<sup>st</sup> ed., Advanced Sensing in Image Processing & IoT, CRC Press, pp. 1-10, 2022. [[Google Scholar](#)] [[Publisher Link](#)]
- [28] Upesh Patel et al., "Dual-Band Compact Split-Ring Resonator-Shaped Fractal Antenna with Defected Ground Plane for Sub-6-GHZ 5G and Global System for Mobile Communication Applications," *International Journal of Communication Systems*, vol. 35, no. 7, 2022. [[CrossRef](#)] [[Google Scholar](#)] [[Publisher Link](#)]
- [29] B. Manichandana et al., "L-Slots Fractal Antenna with DGS for Dual band Applications," *IEEE Wireless Antenna and Microwave Symposium*, Rourkela, India, pp. 1-5, 2022. [[CrossRef](#)] [[Google Scholar](#)] [[Publisher Link](#)]
- [30] Dokrom Froumsia et al., "Miniaturization of Dual Bands Fractal-Based Microstrip Patch Fractal Antenna for X and Ku Bands Application," *The European Physical Journal Plus*, vol. 137, 2022. [[CrossRef](#)] [[Google Scholar](#)] [[Publisher Link](#)]
- [31] Rani Rudrama Kodali, Polepalli Siddaiah, and Mahendra Nanjappa Giriprasad, "Arrow Cross Shape Slotted Fractal Antenna with Enhanced Bandwidth for Wi-Fi/WiMAX/WLAN Applications," *Progress In Electromagnetics Research C*, vol. 119, pp. 115-124, 2022. [[CrossRef](#)] [[Google Scholar](#)] [[Publisher Link](#)]
- [32] Kioumars Pedram et al., "Compact and Miniaturized Metamaterial-Based Microstrip Fractal Antenna with Reconfigurable Qualification," *AEU - International Journal of Electronics and Communications*, vol. 114, 2020. [[CrossRef](#)] [[Google Scholar](#)] [[Publisher Link](#)]